Journal of Solid State Chemistry **147,** 641–646 (1999)
Article ID jssc.1999.8432, available online at http://www.idealibrary.com on IDEAL®

Synthesis and Structures of Yttrium–Transition Metal Sulfates $YM(OH)_3(SO_4)$, M = Ni, Cu

Xiqu Wang, Lumei Liu, and Allan J. Jacobson[1]

Department of Chemistry, University of Houston, Houston, Texas 77204-5641

Received March 12, 1999; in revised form May 28, 1999; accepted June 29, 1999

$YCu(OH)_3(SO_4)$ and $YNi(OH)_3(SO_4)$-I have been synthesized hydrothermally at 380°C at a presssure of 210 MPa. $YCu(OH)_3(SO_4)$ crystallizes in the space group *Pnma* with $a = 13.956(1)$ Å, $b = 6.1349(5)$ Å, and $c = 6.3528(5)$ Å. $YNi(OH)_3(SO_4)$-I crystallizes in the space group $P2_12_12_1$ with $a = 13.335(1)$ Å, $b = 6.1256(5)$ Å, and $c = 6.4830(5)$ Å. The two structures are topologically the same. Different distortions of the CuO_6 and NiO_6 octahedra account for the absence of a center of symmetry in $YNi(OH)_3(SO_4)$-I. Both compounds decompose to form the oxides $Y_2M_2O_5$ when heated to 980–1000°C in air.

Key Words: **hydrothermal synthesis; crystal structure; yttrium copper sulphate; yttrium nickel sulfate.**

INTRODUCTION

Hydrothermal synthesis above the critical point of water (374.1°C, 218.3 atm) has been widely used for the synthesis of metal oxides including compounds with structures related to perovskite (1–4). The perovskite oxide $YCu_3Mn_4O_{12}$ is one example that can be obtained using sulfate sources at 500°C (4). During our investigation of the feasibility for synthesis of complex oxides under somewhat milder conditions near the critical point of water, we have prepared and characterized a number of novel yttrium–transition metal sulfates that contain copper and nickel. These compounds are of interest because superconductivity has been observed recently in some yttrium copper oxides containing sulfate anions (5). Very little is known, however, about the general structural chemistry of yttrium metal sulfates, although a large number of alkali and alkaline–earth metal sulfates have been well characterized (6, 7).

In this paper, we report the syntheses of $YM(OH)_3(SO_4)$, M = Ni, Cu and their characterization by single-crystal X-ray diffraction, infrared (IR) spectroscopy, and thermogravimetric measurements.

[1] To whom correspondence should be addressed. Fax: (713) 743-2787; E-mail: ajjacob@uh.edu.

EXPERIMENTAL

Synthesis

Syntheses were carried out using a Leco HR-1B-2 high-pressure/high-temperature system. Typically, the starting materials were sealed in a flexible Teflon capsule that was subsequently placed in a RENE 41 reaction vessel and heated at 380°C under 210 MPa for 16 h. The products were washed with water, filtered, and dried in air. Pale-blue needles of $YCu(OH)_3(SO_4)$ were obtained as the major phase from reactions starting with $Y(NO_3)_3 \cdot 5H_2O$ (0.37 g, 1 mmol), $CuSO_4 \cdot 5H_2O$ (0.25 g, 1 mmol), and 0.3 mL of 45% KOH aqueous solution. Other phases in the product are blue prisms of $Y_2Cu(OH)_3(SO_4)_2F \cdot H_2O$ and colorless needles of $Y(SO_4)F$ and $Y(OH)(SO_4)$. The fluorine content arises from reactions with the Teflon capsules. Green needles of $YNi(OH)_3(SO_4)$-I were similarly synthesized. They formed together with blue-green polyhedral crystals of $YNi(OH)_3(SO_4)$-II and $Y(SO_4)F$ from reactions starting with $Y(NO_3)_3 \cdot 5H_2O$ (0.37 g, 1 mmol), $NiSO_4 \cdot 6H_2O$ (0.26 g, 1 mmol), and 0.2 mL H_2O. Efforts to synthesize single-phase products by variation of $Y(NO_3)_3/MSO_4$ ratios and water content were not successful.

Characterization

The chemical compositions of the reaction products were analyzed using a JEOL 8600 electron microprobe operating at 15 KeV with a 10 μm beam diameter and a beam current of 30 nA. The measured atomic ratios Y : Cu : S = 1.00 : 0.99 : 1.01 for $YCu(OH)_3(SO_4)$ and Y : Ni : S = 1.00 : 0.96 : 0.96 for $YNi(OH)_3(SO_4)$-I are consistent with the formula ratios derived from the crystal structure refinements.

Infrared spectra were collected with a Galaxy FTIR 5000 spectrometer using the KBr pellet method. Thermogravimetric analyses (TGA) were carried out in a flow of an oxygen/nitrogen gas mixture ($pO_2 = 0.21$ atm) with a heating rate of 1°/min on a TA Instruments TGA 2950 system.

0022-4596/99 $30.00

Samples used for IR spectroscopy and TGA were manually separated from the synthesis products. X-ray powder-diffraction patterns were obtained using Scintag 2000 and Siemens D5000 diffractometers on samples before and after TGA analysis.

Single-crystal X-ray data were measured on a SMART platform diffractometer equipped with a 1 K CCD area detector using graphite-monochromatized Mo$K\alpha$ radiation at room temperature. For each phase, a hemisphere of data (1271 frames at 5 cm detector distance) was collected using a narrow-frame method with scan widths of 0.30° in ω and an exposure time of 30 s/frame. The first 50 frames were remeasured at the end of data collection to monitor instrument and crystal stability, and the maximum correction applied on the intensities was $< 1\%$. The data were integrated using the Siemens SAINT program (8) with the intensities corrected for the Lorentz factor, polarization, air absorption, and absorption due to variation in the path length through the detector faceplate. Absorption corrections were made using the program SADABS (9). The structures were solved by direct methods and refined using SHELXTL (10). All nonhydrogen positions were derived by direct methods and refined anisotropically in the final refinements. The hydrogen atoms were located from Fourier difference maps and refined isotropically with atom distance constraints. Crystallographic and refinement details are summarized in Table 1. Atom positions are given in Table 2 and selected bond lengths and bond angles in Table 3.

TABLE 1
Crystal Data and Structure-Refinement Information for $YCu(OH)_3(SO_4)$ and $YNi(OH)_3(SO_4)$-I

	$YCu(OH)_3(SO_4)$	$YNi(OH)_3(SO_4)$-I
Formula	H_3CuO_7SY	H_3NiO_7SY
F.W.	299.54	294.71
Temperature	293(2) K	293(2) K
Wavelength	0.71073 Å	0.71073 Å
Space group	*Pnma*	$P2_12_12_1$
Unit cell dimensions	$a = 13.9557(12)$ Å	$a = 13.3347(11)$ Å
	$b = 6.1349(5)$ Å	$b = 6.1256(5)$ Å
	$c = 6.3528(5)$ Å	$c = 6.4830(5)$ Å
Volume, Z	543.91(8) Å^3, 4	529.55(7) Å^3, 4
Density (calculated)	3.658 Mg/m^3	3.696 Mg/m^3
Absorption coefficient	14.886 mm^{-1}	14.829 mm^{-1}
Crystal size	$0.40 \times 0.06 \times 0.08$ mm	$0.36 \times 0.10 \times 0.05$ mm
$2\theta_{max}$	57°	57°
Reflections collected	3202	3308
Independent reflections	705 [R(int) = 0.0297]	1205 [R(int) = 0.0449]
Data/restraints/parameters	705/2/63	1205/3/105
Goodness-of-fit on F^2	1.140	1.048
R indices [$I > 2\sigma(I)$]	$R1 = 0.0228$,	$R1 = 0.0256$,
	w$R2 = 0.0575$	w$R2 = 0.0618$
R indices (all data)	$R1 = 0.0240$,	$R1 = 0.0269$,
	w$R2 = 0.0578$	w$R2 = 0.0623$
Extinction coefficient	0.0095(11)	0.0004(9)
Largest diff. peak and hole	0.804 and -0.628 eÅ^{-3}	0.670 and -0.622 eÅ^{-3}

TABLE 2
Atom Coordinates ($\times 10^4$) and Equivalent Isotropic-Displacement Parameters (Å$^2 \times 10^3$) for $YCu(OH)_3(SO_4)$ and $YNi(OH)_3(SO_4)$-I

	x	y	z	U(eq)
		$YCu(OH)_3(SO_4)$		
Y	4180(1)	2500	613(1)	8(1)
Cu	5000	0	5000	11(1)
S	1922(1)	2500	7656(2)	9(1)
O(1)	1360(3)	2500	9614(5)	17(1)
O(2)	2959(2)	2500	8085(5)	17(1)
O(3)	3297(2)	9447(4)	1400(4)	25(1)
O(4)	4635(2)	9909(3)	8026(3)	12(1)
O(5)	4194(2)	2500	4361(5)	11(1)
		$YNi(OH)_3(SO_4)$-I		
Y	9202(1)	2247(1)	3104(1)	8(1)
Ni	10047(1)	−336(1)	7424(1)	8(1)
S	8166(1)	2787(2)	5228(2)	8(1)
O(1)	7207(2)	2008(6)	6004(6)	18(1)
O(2)	8525(3)	1293(6)	3630(6)	18(1)
O(3)	8912(3)	−2809(5)	6963(5)	13(1)
O(4)	8062(3)	5021(5)	4347(6)	14(1)
O(5)	9109(2)	2083(5)	6731(5)	9(1)
O(6)	9699(3)	−200(6)	520(5)	7(1)
O(7)	10500(3)	−59(5)	4361(5)	8(1)

Note. U(eq) is defined as one third of the trace of the orthogonalized U_{ij} *tensor*.

RESULTS AND DISCUSSION

Crystal Structures

The coordination environments of the cations in both structures are shown in Fig. 1. In the structure of $YCu(OH)_3(SO_4)$, the Cu atom is coordinated to four hydroxyl groups at 1.945–1.990 Å and two apical O1 atoms at 2.453 Å, forming an elongated octahedron (Fig. 1a). The strong distortion of the $Cu^{2+}O_6$ octahedra is typical and arises from the Jahn–Teller effect associated with the degenerate electronic ground state of a d^9 metal in an octahedral field (11). The distorted octahedra form edge-sharing chains along [0 1 0] (Fig. 2a). The yttrium atoms are each coordinated by eight oxygen atoms to form strongly distorted bicapped trigonal prisms that link by sharing common edges to form infinite chains parallel to [0 1 0]. The SO_4 tetrahedra are linked to the octahedra to form complex $[Cu(OH)_3SO_4]$ chains. Each apical oxygen atom (O1) at the corner of a CuO_6 octahedron is shared by a SO_4 tetrahedron. The remaining three oxygen atoms of the SO_4 tetrahedron are shared with the yttrium–oxygen polyhedra (Fig. 2a).

Weak hydrogen bonds between O(5) and O(2) ($d_{H(2)-O(2)} = 2.17$ Å; $d_{O(5)-O(2)} = 2.93$ Å) occur in the structure of

TABLE 3
Selected Bond Lengths [Å] and Angles [°] for $YCu(OH)_3(SO_4)$ and $YNi(OH)_3(SO_4)$-I

$YCu(OH)_3(SO_4)$

Y–	Distance			Y–	Distance	
O3	2.297(2) × 2			O4	2.381(2)×2	
O2	2.341(3)			O5	2.382(3)	
O4	2.373(2) × 2					
S–	Distance	Angles				
O3	1.469(2)					
O3	1.469(2)	108.8(2)				
O1	1.471(3)	110.4(1)	110.4(1)			
O2	1.473(3)	107.8(1)	107.8(1)	111.6(2)		
Cu–	Distance	Angles				
O5	1.945(2)					
O5	1.945(2)	180				
O4	1.990(2)	94.34(11)	85.66(11)			
O4	1.990(2)	85.66(11)	94.34(11)	180		
O1	2.453(3)	91.42(9)	88.58(9)	83.16(10)	96.84(10)	
O1	2.453(3)	88.58(9)	91.42(9)	96.84(10)	83.16(10)	180

$YNi(OH)_3(SO_4)$-I

Y–	Distance			Y–	Distance	
O6	2.321(3)			O5	2.356(3)	
O1	2.325(3)			O2	2.373(4)	
O7	2.331(3)			O7	2.377(3)	
O6	2.344(3)			O4	2.418(4)	
S–	Distance	Angles				
O1	1.455(3)					
O2	1.463(3)	109.1(2)				
O4	1.466(4)	110.6(2)	109.1(2)			
O3	1.502(3)	109.1(2)	108.6(2)	110.2(2)		
Ni–	Distance	Angles				
O5	1.990(3)					
O5	2.016(3)	174.70(9)				
O6	2.062(3)	92.8(1)	83.8(1)			
O7	2.083(3)	84.6(1)	99.3(1)	172.0(2)		
O3	2.117(3)	84.8(1)	99.0(1)	86.3(1)	86.0(1)	
O3	2.162(3)	92.9(1)	83.0(1)	90.3(1)	97.4(1)	175.81(8)

$YCu(OH)_3(SO_4)$. Similar weak hydrogen bonds occur in the $YNi(OH)_3(SO_4)$-I structure between O(6) and O(5) and between O(7) and O(3) atoms ($d_{H(2)-O(5)} = 2.24$ Å, $d_{O(5)-O(6)} = 2.86$ Å; $d_{H(3)-O(3)} = 2.30$ Å; $d_{O(7)-O(3)} = 2.93$ Å) (see below).

The structure of $YNi(OH)_3(SO_4)$-I is topologically the same as that of $YCu(OH)_3(SO_4)$. In contrast to the strongly elongated CuO_6 octahedra, however, the NiO_6 octahedra are much less distorted with Ni–O bond lengths between 1.990 and 2.162 Å. The shorter apical Ni–O(1) bonds (2.117–2.162 Å) have a significant influence on the interaction between the octahedral chains and other parts of the structure. In particular, the mirror plane parallel to (0 1 0) is no longer present and the structure becomes noncentrosymmetric ($P2_12_12_1$). If the structure of $YNi(OH)_3(SO_4)$-I were to contain a mirror plane, then, because of the short Ni–O(1) apical distances, substantial changes in Y–O, S–O bond lengths would be needed well beyond those typically observed. Instead, the orientation of the SO_4 tetrahedron adjusts (with the loss of the mirror plane) so that the corresponding Y–O bond lengths change only slightly (≤ 0.12 Å) and the sulfate tetrahedron is only marginally more distorted than in the copper compound. In $YCu(OH)_3(SO_4)$ (Fig. 3a), the SO_4 tetrahedron can be oriented with a mirror plane through the O(1), S, and O(2) atoms without compromising the Y–O, S–O distances because of the rather long Cu–O(1) bonds (2.453 Å). A similar difference in space group between two topologically identical structures that also arises from local coordination requirements of the transition metal occurs for $M_2(OH)VO_4$, $M = Zn$, Ni (12). In this case $Zn_2(OH)VO_4$ crystallizes in the centrosymmetric space group *Pnma* and $Ni_2(OH)VO_4$ in the noncentrosymmetric space group $P2_12_12_1$.

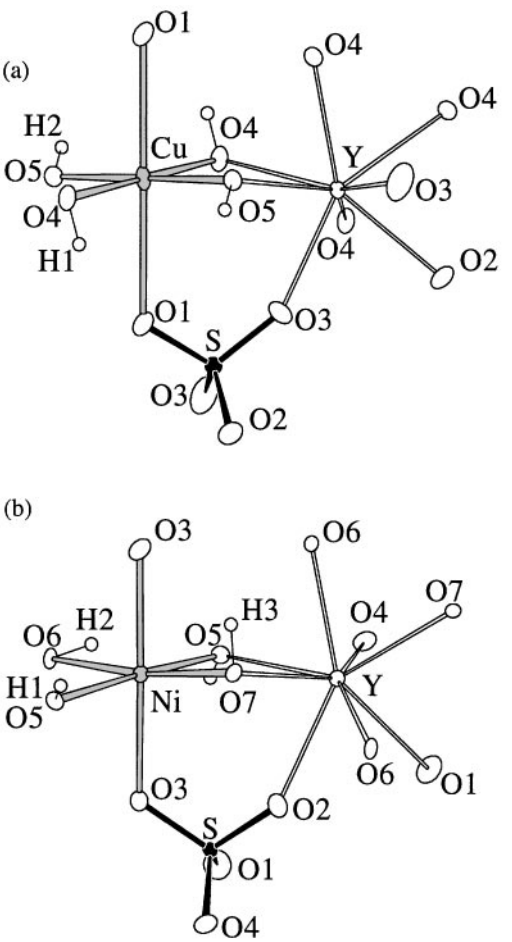

FIG. 1. The local coordination of cations in (a) $YCu(OH)_3(SO_4)$ and (b) $YNi(OH)_3(SO_4)$-I. Thermal ellipsoids are drawn with 50% probability.

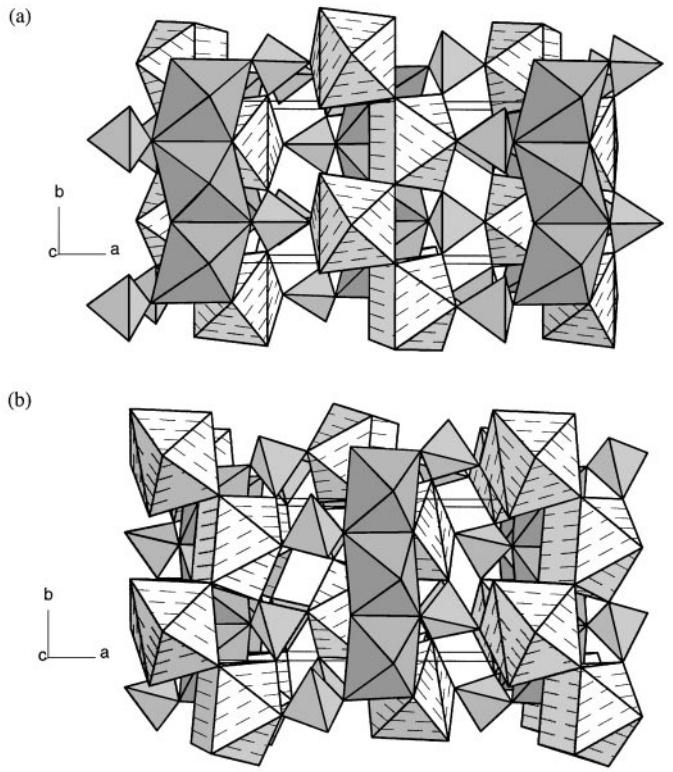

FIG. 2. The structures of (a) $YCu(OH)_3(SO_4)$ and (b) $YNi(OH)_3(SO_4)$-I. YO_8 polyhedra are hatched.

The 1-dimensional $[M(OH)_3SO_4]$ complex chains in the title compounds are uncommon. One known example that contains this kind of chain is the mineral caledonite $Pb_5Cu_2(OH)_6(SO_4)_3CO_3$ where the chains occur with isolated SO_4 and CO_3 groups (13). Bars *et al.* classified these chains as structural-type 7 in their systematic study of $MM'O_4 \cdot 2H_2O$ hydrates where M is octahedrally coordinated and M' tetrahedrally coordinated (14). The 1-dimensional $[M(OH)_3SO_4]$ chains are closely related to several other types of complex chains given in a recent review on sulfate minerals (6) and in broader reviews by Hawthorne on structures containing both tetrahedra and octahedra (15, 16).

Physical Properties

Figure 4 shows the infrared spectra of the two compounds. Relative sharp bands in the range 3448–3609 cm^{-1} correspond to OH groups. Characteristic bands for SO_4 groups in the range 999–1207 cm^{-1} show more features in $YNi(OH)_3(SO_4)$-I than in $YCu(OH)_3(SO_4)$, consistent with the higher symmetry of the latter.

Figure 5 shows the TGA results for both compounds. There are three weight-loss steps for $YCu(OH)_3(SO_4)$. From 450 to 550°C, a weight loss of 8.6% corresponds to dehydration (theoretical 9.0%) according to

$$2YCu(OH)_3(SO_4) \rightarrow Y_2Cu_2O_3(SO_4)_2 + 3H_2O.$$

Between about 750 and 830°C, the second weight loss of 14.2% may be due to the loss of half of the sulfate component in the compound (theoretical 13.4%):

$$Y_2Cu_2O_3(SO_4)_2 \rightarrow Y_2Cu_2O_4(SO_4) + SO_3.$$

The third observed weight loss of 13.3%, which ended at about 980°C, indicates that the compound transformed into $Y_2Cu_2O_5$ by losing all sulfate (theoretical 13.4%):

$$Y_2Cu_2O_4(SO_4) \rightarrow Y_2Cu_2O_5 + SO_3.$$

The total observed (36.1%) and theoretical (35.7%) weight losses are in close agreement. The sample after TGA

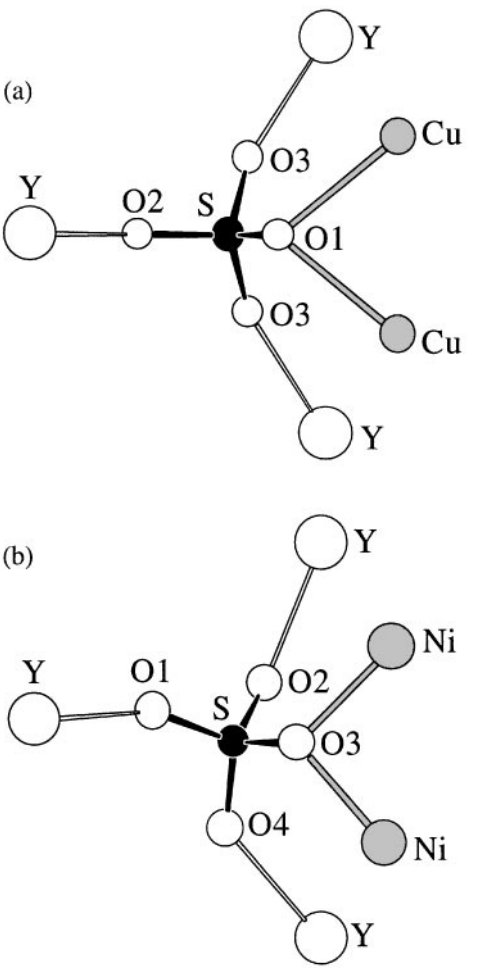

FIG. 3. Orientation of the SO_4 tetrahedra relative to other atoms. (a) $YCu(OH)_3(SO_4)$ and (b) $YNi(OH)_3(SO_4)$-I.

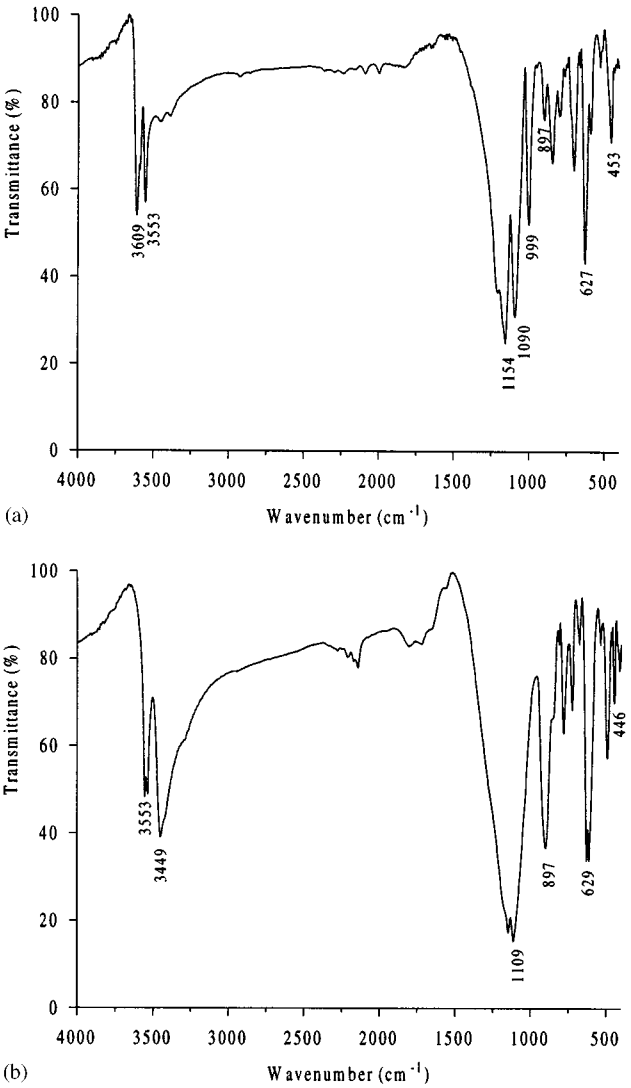

FIG. 4. IR spectra (a) $YNi(OH)_3(SO_4)$-I and (b) $YCu(OH)_3(SO_4)$.

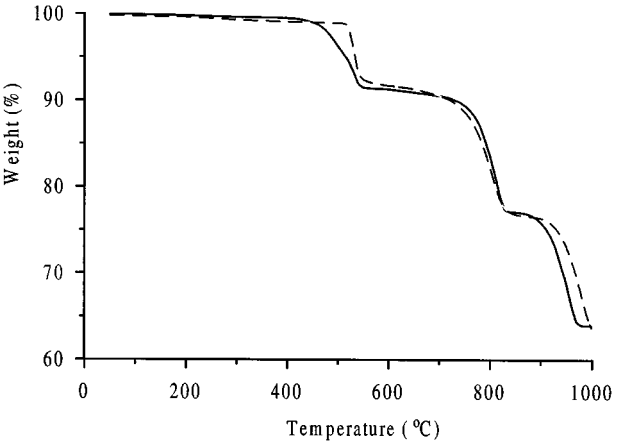

FIG. 5. TGA results. Solid line, $YCu(OH)_3(SO_4)$; dashed line, $YNi(OH)_3(SO_4)$-I.

measurement was confirmed to be $Y_2Cu_2O_5$ by X-ray powder diffraction. The small differences between the theoretical and observed values in the first two steps may indicate that initial dehydroxylation was not complete. Similar thermal behavior was observed for $YNi(OH)_3(SO_4)$-I. The dehydration started at slightly higher temperature and was then faster than for the Cu phase. The final temperature at which the $Y_2M_2O_5$ phase is formed is about 25°C higher for $M = Ni$ than for $M = Cu$ (Fig. 5). As a consequence, for $YNi(OH)_3(SO_4)$-I, no plateau was reached at the upper temperature limit of the instrument of 1000°C. No further weight change was observed when the sample was held at 1000°C for 7 h. The final weight of the sample at this temperature corresponds to the transformation of the sulfate into the oxide $Y_2Ni_2O_5$.

CONCLUSIONS

The yttrium–transition metal sulfates $YCu(OH)_3(SO_4)$ and $YNi(OH)_3(SO_4)$-I have been synthesized hydrothermally at temperatures just above the critical point of water. The two compounds have topologically equivalent structures. The structure $YNi(OH)_3(SO_4)$-I is noncentrosymmetric but $YCu(OH)_3(SO_4)$ is centrosymmetric. This difference arises because of the axial distortion of the CuO_6 octahedron due to the Jahn–Teller effect. Both compounds decompose to form the oxides $Y_2M_2O_5$ at temperatures of 980–1000°C in air.

ACKNOWLEDGMENTS

We thank the National Science Foundation (DMR9214804) and the R. A. Welch Foundation for financial support. This work made use of MRSEC/TCSUH Shared Experimental Facilities supported by the National Science Foundation under Award DMR-9632667 and the Texas Center for Superconductivity at the University of Houston.

REFERENCES

1. K. Byrappa, *in* "Handbook of Crystal Growth" (D. T. J. Hurle, Ed.), Vol. 2, p. 466. Elsevier Science, Amsterdam, 1994.
2. L. N. Demianets and A. N. Lobachev, *in* "Current topics in Materials Science" (E. Kaldis, Ed.), Vol. 7, p. 483. North-Holland, Amsterdam, 1981.
3. G. Demazeau, J-M. Millet, C. Cros, and A. Largeteau, *J. Alloys Comp.* **262/263,** 271 (1997).
4. A. Collomb, D. Samaras, J. L. Buevoz, J. P. Levy, and J. C. Joubert, *J. Magn. Magn. Mater.* **40,** 75 (1983).
5. P. R. Slater, C. Greaves, M. Slaski, and C. M. Muirhead, *Physica C* **208,** 193 (1993).
6. D. Yu. Pushcharovsky, J. Lima-de-Faria, and R. K. Rastsvetaeva, *Z. Kristallogr.* **213,** 141 (1998).

7. K. M. Eriksen, K. Nielsen, and R. Fehrmann, *Inorg. Chem.* **35,** 480 (1996).
8. "SAINT, Version 4.05," Siemens Analytical X-ray Instruments, Madison, WI, 1995.
9. G. M. Sheldrick, "SADABS Program," University of Göttingen, 1995.
10. G. M. Sheldrick, "SHELXTL, Version 5.03," Siemens Analytical X-ray Instruments, Madison, WI, 1995.
11. P. C. Burns and F. C. Hawthorne, *Canad. Miner.* **34,** 1089 (1996).
12. X. Wang, L. Liu, and A. J. Jacobson, *Z. Anorg. Allg. Chem.* **624,** 1977 (1998).
13. C. Giacovazzo, S. Menchetti, and F. Scordari, *Acta Cryst. B* **29,** 1986 (1973).
14. O. Bars, J. Y. L. Marouille, and D. Grandjean, *Acta Cryst. B* **37,** 2143 (1981).
15. F. C. Hawthorne, *Z. Kristallogr.* **192,** 1 (1990).
16. F. C. Hawthorne, *Acta Cryst. B* **50,** 481 (1994).